JOURNAL OF SOLID STATE CHEMISTRY 70, 295–302 (1987)

Ferro- and Antiferromagnetism in Oxychalcogenides $LnCrOX_2$ (Ln = La or Nd and X = S or Se)*,[1]

M. WINTENBERGER, J. DUGUE, M. GUITTARD, NGUYEN HUY DUNG, AND VO VAN TIEN

Laboratoire de Chimie Minérale Structurale, Laboratoire associé au CNRS UA 200, Faculté des Sciences Pharmaceutiques et Biologiques de Paris V, 4, Avenue de l'Observatoire 75270 Paris, Cedex 06, France

Received October 15, 1986

The two isomorphous compounds $LaCrOS_2$ and $LaCrOSe_2$ are ferromagnetic (T_c = 35 and 51 K, respectively). This implies ferromagnetic super-superexchange interactions. $NdCrOS_2$ is antiferromagnetic (T_N = 72 K) and undergoes a spin–flop transition (H_c = 54 KOe at 20 K). The study of the thermal variation of Cr^{3+} and Nd^{3+} magnetic moments below T_N allows a rough estimate of the Cr–Nd and Cr–Cr exchange fields ratio (~0.1). © 1987 Academic Press, Inc.

Introduction

After having unexpectedly found ferromagnetism in $LaCrOS_2$ (*1*), we investigated the magnetic properties of some related compounds, namely $LaCrOSe_2$ and $NdCrOS_2$. The results of magnetization measurements and neutron diffraction are reported here, but some features of the crystal structures, which seem to be relevant to the magnetic interactions, will be described first.

Crystal Structures

The space groups and lattice parameters are given in Table I.

The structure of $LaCrOS_2$ (space group *Pbnm*) was determined by Dugué *et al.* (*2*). In (*3*) it was stated that $LaCrOSe_2$ was isomorphous to $CeCrOS_2$ (space group $B2/m$), and thus to $NdCrOS_2$. However, the examination of Weissenberg photographs shows that $LaCrOSe_2$ has orthorhombic symmetry, with the systematic extinctions of group *Pbnm*, and is isomorphous to $LaCrOS_2$.

We performed a refinement of the structure of $NdCrOS_2$ from single crystal data (745 reflections, R_F = 2.4%). It gives the atomic coordinates of Table II. They are practically identical to those of $CeCrOS_2$.

The structure of $LaCrOS_2$ is shown in Fig. 1a. The Cr atoms are all equivalent. They are surrounded by S_5O octahedra, which share S–S edges to form double chains running parallel to the c axis. Between these chains are seen zigzag $(La–O)_n^{n+}$ double chains, also parallel to the c axis. The La–O distances are 2.47 and 2.33 Å, the last one being among the shortest known La–O distances. Some authors (*4*, *5*) think that such La–O bonds are partially

* Dedicated to Dr. Hans Nowotny.
[1] Dedicated by Prof. J. M. Flahaut.

0022-4596/87 $3.00

TABLE I

SPACE GROUPS AND LATTICE PARAMETERS OF THE THREE COMPOUNDS

Compound	Space group	a	b	c	γ
$LaCrOS_2$	*Pbnm*	11.23	8.43	3.71	
$LaCrOSe_2$	*Pbnm*	11.54	8.55	3.82	
$NdCrOS_2$	*B2/m*	11.43	7.89	3.67	90°2

TABLE II

ATOMIC COORDINATES OF $NdCrOS_2$

Atom	Site	Symmetry	x	y	z
Nd	4i	m	0.23421(3)	0.20694(4)	1/2
CrI	2a	$2/m$	0	0	0
CrII	2d	$2/m$	1/2	1/2	0
O	4i	m	0.1660(4)	0.0610(5)	0
S_I	4i	m	0.4556(1)	0.1986(2)	0
S_{II}	4i	m	0.1366(1)	0.4697(2)	0

covalent and that $(La–O)_n^{n+}$ groups are really polycations. This could make them efficient in the propagation of exchange interactions.

Inside the Cr^{3+} chains there are Cr–S–Cr magnetic exchange paths with bond angles near 90° (from 87 to 99°). In this geometry there is a competition between antiferromagnetic direct Cr–Cr interactions and ferromagnetic superexchange, so the resultant is of medium strength, and often ferromagnetic. As for the interchain interactions they are of super-superexchange type, via two anions and a La^{3+} ion, so they are probably weaker than the intrachain ones. Their sign cannot be easily predicted. The paths are of three types: (a) with two La–O bonds (a full double La–O chain), (b) with two La–S bonds, and (c) with one La–O and one La–S bond. Type (a) paths connect the Cr double chains inside (100) planes. For interplane coupling (b) and (c) types only are available (not (c) only as was stated in Ref. (*1*)).

The structure of $NdCrOS_2$ is shown in Fig. 1b. There are two inequivalent Cr sites. One is surrounded by an S_4O_2 octahedron, and the other by an S_6 one. These octahedra form chains parallel to the c axis by edge sharing. The chains are connected by shared octahedral vertices to form planes parallel to (100). The Cr–S–Cr bond angles are 95 and 99° for the case of shared edges and 125° for the case of shared vertices. The sign of the magnetic exchange interaction for this last angle value cannot be predicted from simple arguments. Nd atoms are situated between the above planes.

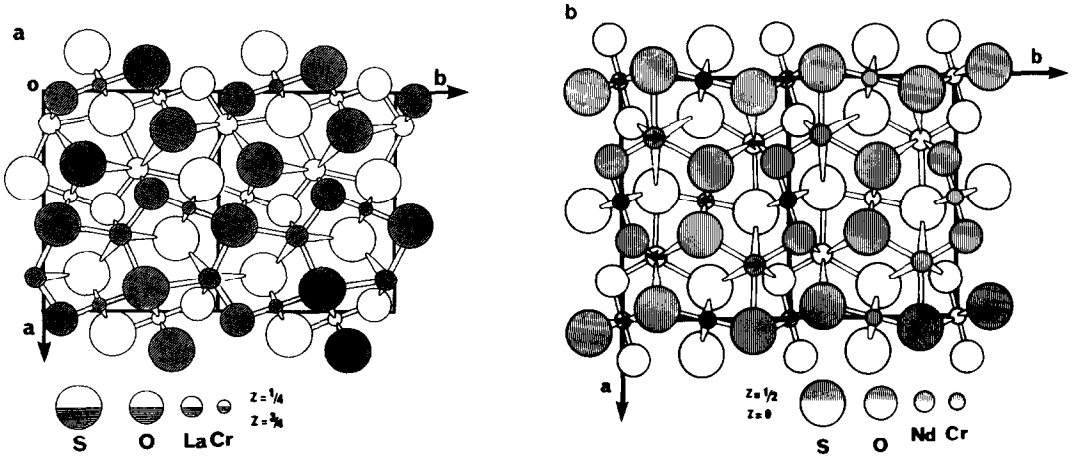

FIG. 1. Crystal structures of (a) $LaCrOS_2$ and (b) $NdCrOS_2$. Two unit cells are drawn in each case.

TABLE III

TYPE OF MAGNETISM, ORDERING TEMPERATURE, ASYMPTOTIC CURIE TEMPERATURE, EFFECTIVE MOMENT, AND SATURATION MAGNETIZATION OF THE THREE COMPOUNDS

Compound	Type	$T_{C,N}$	θ_p	$(\Sigma\mu_{eff}^2)^{1/2}$ Obs.	Calc.	$\sigma \cdot \mu_{B/Cr}$
$LaCrOS_2$	F	35	55	3.8	3.87	2.6
$LaCrOSe_2$	F	51	90	4	3.87	2.25
$NdCrOS_2$	AF	72	72	5.15	5.34	—

It is possible in this structure too, to visualize double Nd–O chains with Nd–O distances 2.30 and 2.40 Å.

To summarize this description, one could anticipate ferromagnetic intrachain Cr–Cr coupling, and weaker interplane Cr–Cr coupling of unknown sign, and also rather weak interchain coupling in the La compounds.

Magnetic Properties

Most measurements were made at Laboratoire Louis Néel in Grenoble, by the axial extraction method, up to 60 KOe and down to 4.2 K.

Characteristic magnetic data are collected in Table III. The three compounds have positive paramagnetic Curie temperatures θ_p, which means that the ferromagnetic interactions are dominant.

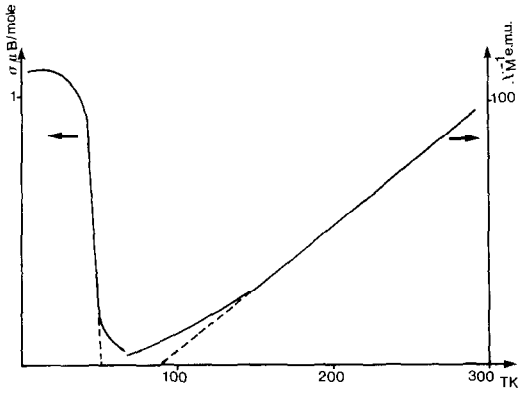

FIG. 2. Inverse susceptibility and low field magnetization of $LaCrOSe_2$ as functions of temperature.

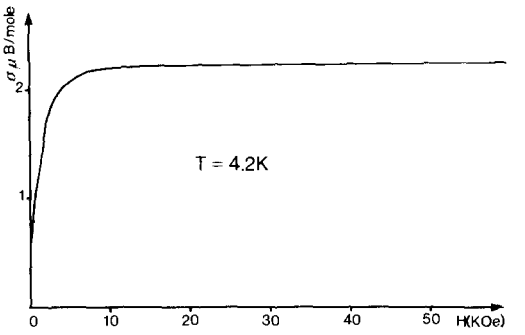

FIG. 3. Magnetization of $LaCrOSe_2$ as a function of magnetic field at 4.2 K.

The details about the ferromagnetism of $LaCrOS_2$ were given in (*1*).

$LaCrOSe_2$ too is ferromagnetic. Its inverse susceptibility χ^{-1} and its magnetization σ as functions of temperature T are shown in Fig. 2, and a magnetization versus magnetic field curve is shown in Fig. 3. In Fig. 2 one can see that short range order seems to persist in a large temperature range above T_c. The same is true, to a lesser extent, for $LaCrOS_2$ (*1*).

$NdCrOS_2$ is antiferromagnetic in moderate fields, as can be seen from the thermal variation of χ (Fig. 4). Below 72 K the susceptibility decreases, slowly first and then more rapidly, showing that Nd is ordered. Magnetization isotherms were recorded at

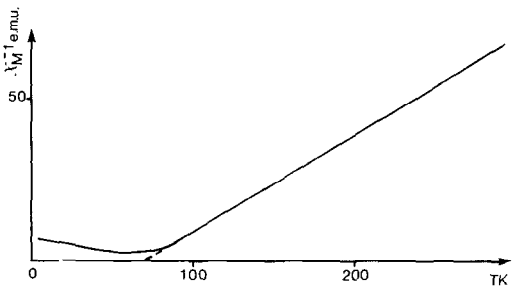

FIG. 4. Inverse susceptibility of $NdCrOS_2$ as a function of temperature.

small temperature intervals from 4.2 to 100 K. For clarity, only three isotherms are drawn in Fig. 5. Between 20 K and T_N the curves have a weak but distinct anomaly indicating a spin–flop transition. As the measurements were made on polycrystalline samples the determination of the critical field H_c for spin–flopping cannot be precise. However, the curve H_c versus T deduced from these measurements (Fig. 6) shows a regular decrease of H_c with increasing T up to 65 K. H_c does not seem to go to zero at T_N but a more precise description of the magnetic properties, particularly near T_N, would require measurements on single crystals. Saturation is not reached at any temperature. Above T_N the magnetization does not increase linearly with magnetic field, its variation is similar to that of a ferromagnet just above T_C. This effect of the strong ferromagnetic interactions can still be seen at 100 K.

Magnetic Structures

Neutron diffraction results about La $CrOS_2$ are given in (*1*). A neutron diffraction study of $LaCrOSe_2$ did not seem useful.

A detailed study of $NdCrOS_2$ at various temperatures was made on the two-axis

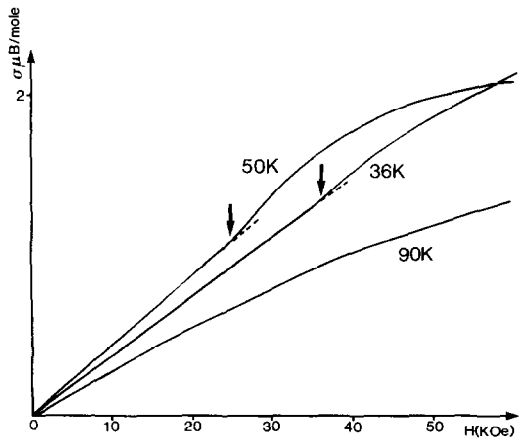

FIG. 5. Some magnetization isotherms of $NdCrOS_2$.

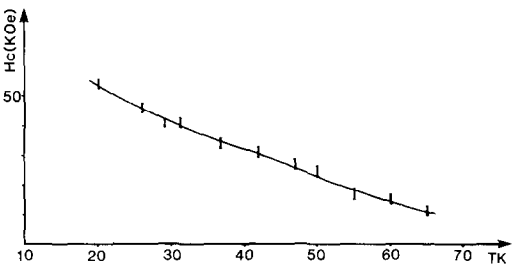

FIG. 6. $NdCrOS_2$ spin–flop critical field as a function of temperature.

spectrometer Pyrrhias at Laboratoire Léon Brillouin. The wavelength was 2.45 Å. Figure 7 shows the diagrams recorded at 1.5, 40, and 300 K. Two weak lines at Bragg angles $\theta = 11°4$ and $16°2$ could not be identified. The weak line at $\theta = 23°9$ is probably due to some unreacted Nd_2O_2S.

The room temperature results show good agreement between observed and calculated nuclear intensities (Table IV).

TABLE IV

CALCULATED AND OBSERVED NUCLEAR INTENSITIES OF $NdCrOS_2$[a]

hkl	$I_{calc.}$	$I_{obs.}$
010	49.5	45.7
200	17.45	19.7
$\begin{pmatrix}210\\2\bar{1}0\end{pmatrix}$	19.95	19.6
$\begin{pmatrix}220\\2\bar{2}0\end{pmatrix}$	19.15	17.26
$\begin{pmatrix}111\\1\bar{1}1\end{pmatrix}$	30.3	32.9
400	7.6	7.5
$\begin{pmatrix}410\\4\bar{1}0\end{pmatrix}$	23.3	22.3
$\begin{pmatrix}030\\301\\121\\1\bar{2}1\end{pmatrix}$	73.6	65
$\begin{pmatrix}311\\3\bar{1}1\end{pmatrix}$	60.15	61.7
$\begin{pmatrix}420\\4\bar{2}0\end{pmatrix}$	32.13	36.5
040	12.6	17.6

[a] $I = pF_N^2 L(\theta)$.

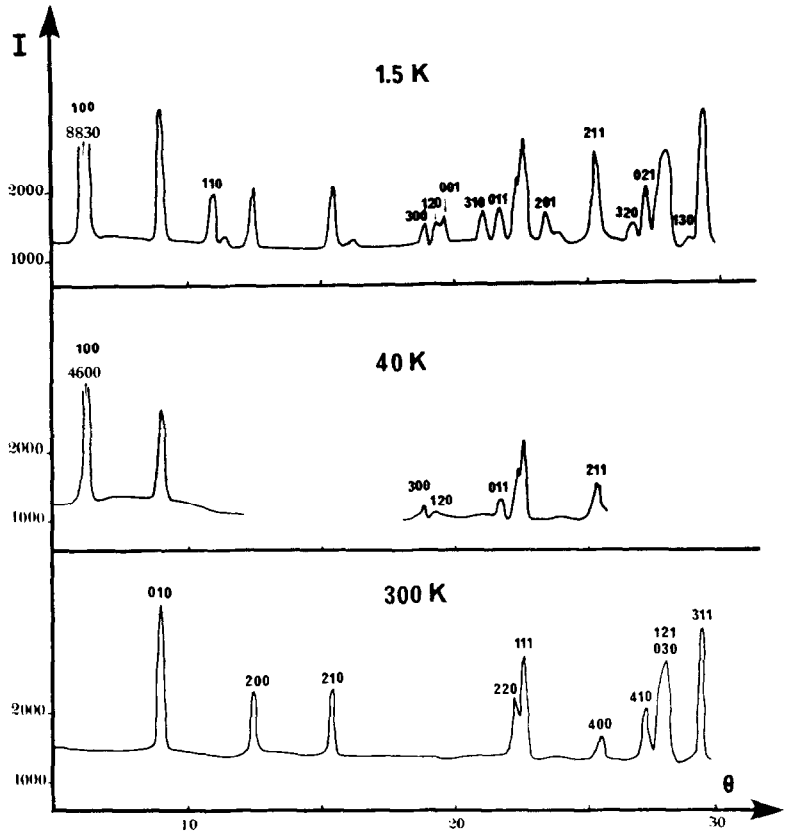

FIG. 7. Neutron diffraction diagrams of $NdCrOS_2$. The scale factor of the 40 K diagram is different from that of the other two. $\lambda = 2.45$ Å.

Lines of magnetic origin are seen in the 40 K diagram. They can be indexed on the basis of the chemical unit cell ($\mathbf{k} = 0$) and obey the conditions $h + l$ and $h + k$ odd. (As seen in Fig. 8, with an increased counting time a very weak (110) line is still visible at this temperature.)

On the 1.5 K diagram additional reflections still belonging to $\mathbf{k} = 0$, are found, again with $h + l$ odd but now with $h + k$ even.

So in both cases the magnetic space group is B_p . . . , and only four irreducible representations of $B2/m$ have to be considered for the symmetry analysis. They are written in Table V, together with the allowed magnetic modes (we call Nd_1 and Nd_2 the Nd atoms on sites x, y, 1/2 and $-x$, $-y$, 1/2 and $\mathbf{F} = \mathbf{S}_{Nd_1} + \mathbf{S}_{Nd_2}$, $\mathbf{A} = \mathbf{S}_{Nd_1} - \mathbf{S}_{Nd_2}$).

As both the **F** and **A** modes contribute to $h + k = 2n$ intensities, $\mathbf{F} = \mathbf{A} = 0$ if $h + k =$

TABLE V

IRREDUCIBLE REPS OF $2/m$ FOR $\mathbf{k} = 0$ AND ALLOWED MODES

	E	$2z$	$\bar{1}$	m	Cr_I	Cr_{II}	Nd
$\Gamma_1 g$	1	1	1	1	Sz	Sz	Fz
$\Gamma_2 g$	1	$\bar{1}$	1	$\bar{1}$	Sx, Sy	Sx, Sy	Fx, Fy
$\Gamma_3 u$	1	$\bar{1}$	$\bar{1}$	1	—	—	Az
$\Gamma_4 u$	1	1	$\bar{1}$	$\bar{1}$	—	—	Ax, Ay

[a] Nd_1 on x, y, 1/2; Nd_2 on $\bar{x}$, $\bar{y}$, 1/2; $\mathbf{F} = \mathbf{S}_{Nd_1} + \mathbf{S}_{Nd_2}$; $\mathbf{A} = \mathbf{S}_{Nd_1} - \mathbf{S}_{Nd_2}$.

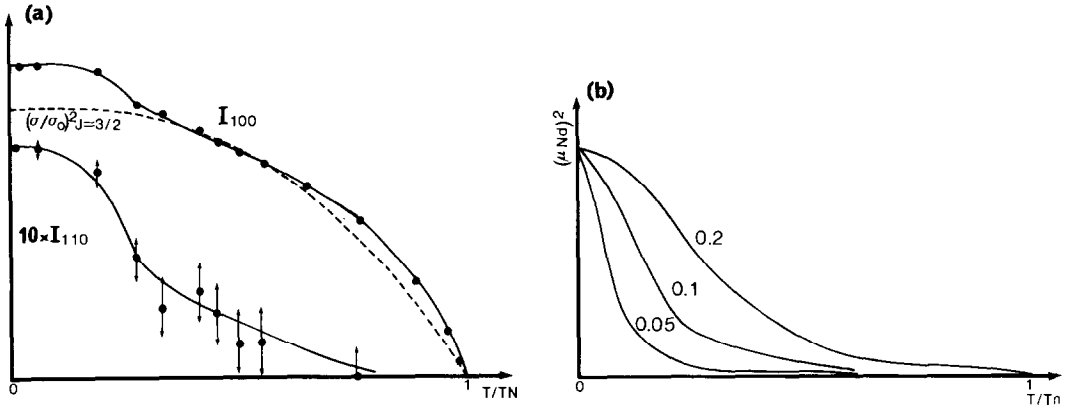

FIG. 8. (a) Temperature dependence of the intensities of (100) and (110) reflections. The curve $(\sigma/\sigma^0)^2$ for $J = 3/2$, normalized to the Cr contribution, is drawn for comparison (dotted line). (b) Theoretical variation of $(\mu_{Nd})^2$ with temperature in the molecular field model.

$2n$ are absent and at 40 K there is practically no contribution from Nd.

In all the following it will be assumed that $\mu_{Cr_I} = \mu_{Cr_{II}}$. The mode $\mathbf{S}_{Cr_I} + \mathbf{S}_{Cr_{II}}$ would give lines with $h + k = 2n$ only. Finally the only mode present at 40 K is $\mathbf{S}_{Cr_I} - \mathbf{S}_{Cr_{II}}$. The magnetic structure consists of ferromagnetic planes parallel to (100), these planes being coupled antiferromagnetically.

From the comparison of calculated and observed intensities (Table VI) one gets $\mu_{Cr} = 1.7\ \mu_B$, the moments being along the b axis or close to it. (Note that for the Cr sites $F(hkl) = F(h\bar{k}l)$.) The structure belongs to representation Γ_{2g}, and the magnetic space group is B_p2'/m'. We use for Cr^{3+} the magnetic form factor of Watson and Freeman (*6*).

TABLE VI

CALCULATED AND OBSERVED MAGNETIC INTENSITIES OF $NdCrOS_2$ AT 40 K[a]

hkl	$I_{calc.}$	$I_{obs.}$
100	73.4	73
300	6.4	3.9
120	1.3	1.3
011	7.3	6.7
211	9.6	12.3

[a] $I = p\ 0.27^2 < \sin^2\alpha > F_M^2\ L(\theta)$; $\mu_{Cr} = 1.7\ \mu_B$.

It seems natural to assume that the lines with $h + k = 2n$ which are seen at 1.5 K are due to Nd ordering. With this assumption one finds that Nd orders with a mode **F** along the b axis or close to it. This mode belongs to representation Γ_{2g} like the $T = 40$ K structure. Using for Nd the experimental magnetic form factor shown in (*7*), one gets $\mu_{Nd} = 1.85 \pm 0.15\ \mu_B$ at 1.5 K (Table VII). An attempt to add a contribution from Cr to these lines (mode $\mathbf{S}_{Cr_I} + \mathbf{S}_{Cr_{II}}$) cannot improve the agreement between measurements and calculation.

The parameters which remain unknown at this stage are the relative directions of Cr and Nd moments and the ratio μ_{Cr}/μ_{Nd}. The first one is easily determined: the moments of Cr_I (0, 0, 0) and Nd (x, y, 1/2) are parallel (the structure being described by $\mathbf{S}_{Cr_I} - \mathbf{S}_{Cr_{II}} + \mathbf{F}_{Nd}$). The best agreement between $I_{obs.}$ and $I_{calc.}$ (Table VII) is obtained for $\mu_{Cr}/\mu_{Nd} = 1.3$, which gives $\mu_{Cr} = 2.4 \pm 0.2\ \mu_B$. The magnetic structure is indicated in Fig. 1b.

TABLE VII

CALCULATED AND OBSERVED MAGNETIC INTENSITIES OF $NdCrOS_2$ AT 1.5 K[a]

$h + k = 2n$			$h + k = 2n + 1$		
hkl	$I_{calc.}$	$I_{obs.}$	hkl	$I_{calc.}$	$I_{obs.}$
$\begin{pmatrix}110\\1\bar{1}0\end{pmatrix}$	16.9	14.2	100	163	163
			300	7	5
001	8.6	9.6	$\begin{pmatrix}120\\1\bar{2}0\end{pmatrix}$	2.7	4.3
$\begin{pmatrix}310\\3\bar{1}0\end{pmatrix}$	10.4	13.4			
			$\begin{pmatrix}011\\0\bar{1}1\end{pmatrix}$	8.1	13.9
201	11.6	13.6			
021	3.5	3			
			$\begin{pmatrix}211\\2\bar{1}1\end{pmatrix}$	30	42
$\begin{pmatrix}130\\1\bar{3}0\end{pmatrix}$	0.2	—			
			$\begin{pmatrix}320\\3\bar{2}0\end{pmatrix}$	8.7	10

[a] I same as in Table VI; $\mu_{Cr} = 2.4\ \mu_B$; $\mu_{Nd} = 1.85\ \mu_B$.

The temperature dependence of μ_{Cr} and μ_{Nd} was studied by measuring the intensities of the strong (100) line (for which the Cr contribution is dominant) and of the weak (110) reflection (due to Nd only). In spite of long counting times, the latter was obtained with a poor precision. The results are shown in Fig. 8a.

This study also allowed us to check that the linewidth of (100) remains constant from 1.5 to 65 K.

Discussion

For the La compounds the occurrence of ferromagnetic Cr–Cr interactions through shared edges of octahedra is not surprising, but these interactions alone cannot ensure 3D-order, which is due also to long range interactions of super-superexchange type. If not all, some of the latter at least are thus necessarily ferromagnetic.

For $NdCrOS_2$ the present work brings some information about the Nd^{3+} ion and about Nd–Cr interactions.

The moment of Nd^{3+} at 1.5 K is only 1.85 μ_B, instead of 3.27 μ_B for the free ion. This is due to the splitting of the $^4I_{9/2}$ level into Kramers doublets by the crystal field of Cs symmetry. The resulting anisotropy is reflected in the spin–flop behavior and seems to remain large even at temperatures near T_N (Fig. 6).

The magnetic structure belongs to the same magnetic space group (B_p2'/m') from 1.5 K to T_N, and the direction of the magnetic moments does not vary with temperature T either. From these facts, and from the variation of μ_{Nd} with T, one concludes that there is only one transition temperature $T_N = 72$ K for $NdCrOS_2$, even though the magnetic lines due to Nd cannot be seen for $T > 40$ K. This means that Cr–Nd exchange interactions are a substantial fraction of Cr–Cr ones. Assuming that Nd–Nd interactions can be neglected, we tried to make an approximate evaluation of the ratio of the exchange fields A, due to Cr–Cr interactions, and A' due to Cr–Nd interactions, using the following molecular field equations:

$$\mu_{Cr} = 2.4B_{3/2}\left(2.4\,\frac{A\mu_{Cr} + A'\mu_{Nd}}{kT}\right)$$

$$\mu_{Nd} = 1.85B_{1/2}\left(1.85\,\frac{A'\mu_{Cr}}{kT}\right).$$

In these formulas we made the simplifying assumption that for Nd^{3+} the ground level alone is populated up to T_N, which is certainly not true, so that we can only obtain a very rough approximation. The equations were solved by the graphical method of Néel (*8*) considering the values $A'/A = 0.05$, 0.1, and 0.2. This gives the values of μ_{Cr} and μ_{Nd} as functions of T/T_N. In each case μ_{Cr} follows the normal curve σ/σ° for $S = 3/2$. The calculated values of $(\mu_{Nd})^2$,

shown in Fig. 8b, allow a direct comparison with observed neutron intensities. An agreement between calculated and experimental curves is found for $A'/A = 0.2$. However, as the intrinsic moment of Nd^{3+} certainly increases with T, A'/A is more probably of the order 0.1. In this respect $NdCrOS_2$ is similar to the rare earth garnets for which A'/A is 0.1 (9) rather than to the rare earth orthochromites for which A'/A is 10^{-3} (*10*).

Finally, we tried to find how Cr and Nd remain coupled together after the spin–flop transition. Unfortunately the saturation is far from being reached at low temperature. The most favorable temperature is 50 K (Fig. 6), where the magnetization nearly reaches a plateau at 2.1 μB for $H > 50$ KOe. At this temperature the Cr^{3+} moment would be only 1.9 μB, so it seems that Cr and Nd with parallel moments remain coupled after the spin–flop transition, while antiferromagnetic Nd–Cr couplings are broken. But low temperature, high field measurements would be necessary to confirm this assumption.

In summary, this work has evidenced two new ferromagnetic compounds, La $CrOS_2$ and $LaCrOSe_2$, implying the existence of long range ferromagnetic exchange interactions. It also has evidenced relatively strong Cr–Nd superexchange interactions, ferro- as well as antiferromagnetic, in $NdCrOS_2$.

Acknowledgments

We heartily thank M. Barlet of Laboratory Louis Néel for his contribution to the magnetic measurements, and Y. Allain of Laboratory Leon Brillouin for his help during neutron diffraction experiments.

References

1. M. Wintenberger, T. Vo Van and M. Guittard, *Solid State Comm.* **53,** 227 (1985).
2. J. Dugué, T. Vo Van, and J. Villers, *Acta Crystallogr. B* **36,** 1291 (1980).
3. Vo Van and D. Nguyen Huy, *C.R. Acad. Sci. Paris II* **293,** 933 (1981).
4. P. Caro, *C.R. Acad. Sci. Paris C* **262,** 992 (1966).
5. C. K. Jørgensen, R. Pappalardo, and J. Flahaut, *J. Chim. Phys.*, 444 (1965).
6. R. E. Watson, and A. J. Freeman, *Acta Crystallogr.* **14,** 27 (1961).
7. M. Blume, A. J. Freeman, and R. E. Watson, *J. Chem. Phys.* **37,** 1245 (1962).
8. L. Néel, *Ann. Phys.* **3,** 137 (1948).
9. L. Néel, R. Pauthenet, and B. Dreyfus, *Prog. Low. Temp. Phys. IV,* 344 (1964).
10. J. Sivardière, Thesis, AO CNRS 1686, Grenoble (1970).